

Article

On Mautner-Type Probability of Capture of Intergalactic Meteor Particles by Habitable Exoplanets

Andjelka B. Kovačević 

Department of Astronomy, Faculty of Mathematics, University of Belgrade, Studentski trg 16, 11000 Belgrade, Serbia; andjelka@matf.bg.ac.rs

Received: 28 June 2019; Accepted: 10 July 2019;

First Version Published: 15 July 2019 (doi:10.3390/sci1020040)



Abstract: Both macro and microprojectiles (e.g., interplanetary, interstellar and even intergalactic material) are seen as an important vehicle for the exchange of (bio)material within our solar system as well as between stellar systems in our Galaxy. Accordingly, this requires estimates of the impact probabilities for different source populations of projectiles, specifically for intergalactic meteor particles which have received relatively little attention since considered as rare events (discrete occurrences that are statistically improbable due to their very infrequent appearance). We employ the simple but yet comprehensive model of intergalactic microprojectile capture by the gravity of exoplanets which enables us to estimate the map of collisional probabilities for an available sample of exoplanets in habitable zones around host stars. The model includes a dynamical description of the capture adopted from Mautner model of interstellar exchange of microparticles and changed for our purposes. We use statistical and information metrics to calculate probability map of intergalactic meteorite particle capture. Moreover, by calculating the entropy index map we measure the concentration of these rare events. By adopting a model from immigration theory, we show that the transient distribution of birth/death/immigration of material for the simplest case has a high value.

Keywords: astrobiology; extrasolar planets; intergalactic meteor particle

1. Introduction

The Universe has been generating random events, which can be very unpredictable and affect planetary environments in different ways. Probability distributions of such events are often observed to have power-law tails [1]. One of many examples include the natural transport of material within our Solar system.

Molecules, excluding the most stable as polycyclic aromatic hydrocarbons, are quickly (10–10,000 years) destroyed by e.g., the UV radiation of stars [2,3]. So defensive vessels are required that would protect and transport them across space. Interestingly, the recent observations accumulate evidence about interstellar, and even intergalactic transport of material. For example, observation of the first known Interstellar Object (ISO) 1I/2017 U1 Oumuamua by the Pan-STARRS telescope in October 2017 [4] has given a new input to a broad topic about the possibility of natural transport of solid material and complex molecules through space (see [5] and references therein). This object was the first ISO observed on macro scale. Almost two decades ago, Taylor et al. [6] discovered interstellar dust entering the Earth atmosphere. Ten years later, Afanasiev et al. [7] detected a centimeter-size Intergalactic meteor particle (IMP). This IMP hit the Earth atmosphere with a hypervelocity 300 km s^{-1} . However, only about 1% of meteors have velocities above 100 km s^{-1} , and no previous meteor observations have confirmed velocities of several hundred km s^{-1} [8]. Afanasiev et al. [7] calculated that IMP was

0.01 cm in size and its mass was about 7×10^{-6} g. This IMP was two orders of magnitude larger than common interstellar dust grains in our Galaxy. Additionally, its spectral features were a typical for the materials being exposed to the temperatures of 15,000–20,000 K. Its radiant appeared to coincide with the apex of the motion of the Solar system toward the centroid of the Local Group of galaxies. The authors calculated that average density of IMP population in the Earth's vicinity could exceed 2.5×10^{-31} g cm⁻³. If the extragalactic dust is uniformly distributed over the entire volume of Local Group, with above density, Afanasiev et al. [7] claimed that the total mass of the dust is about of 1% of the total mass of the Local Group. Moreover, their followup observations identified a dozen IMP candidates consistent with previous one, which is in disagreement with the lack of any evidence from other optical meteor observatories (see e.g., [9]). Nevertheless, Afanasiev et al. [7] study shows that the existence of meteors of galactic velocities cannot completely be ruled out.

Linking the facts that our Milky Way galaxy is home to $\sim 10^{10}$ exoplanets [10] and above mentioned possible influx of IMP on our planet, naturally arises question about probability of migration of material in our Local Group, particularly, those molecules which can be useful for life development on planets.

Although the trade of viable organisms between planets in our system is an open question [11], the exchange of molecular species may be much more likely [12]. It is believed that material exchange between rocky planets could amplify chemical space within the planetary system [13]. As transfer vehicles were suggested meteoroids (particles from 1 μ m up to 1 cm), meteorites (1 cm up to 10 m), comet's nuclei and asteroids. Moreover, ISO objects [14] and even planets can serve as transporters of complex molecules through space based on the fact that recently has been detected an extragalactic planetary companion around HIP 13044 in our Galaxy [15].

Interstellar and intergalactic meteoroids, able to transfer molecules, are very difficult to observe. Therefore, we do not have a reliable information about their population density and dynamics. Unlike them, interstellar dust grains ($\lesssim 1 \mu$ m in size) have been intensively studied for a long time [16]. Dust grains mainly flow with interstellar gas. For example, due to non even distribution of brighter star in the Galaxy, dust grains can have speed up to 2 to 10 km s⁻¹ relative to the gas due to the radiation pressure [17]. Betatron mechanism can accelerate them up to 30 to 100 km s⁻¹. Finally, dust grains and gas can be expelled into the intergalactic space [18,19], if galaxy passes episodes of violent star formation. If such particle end up in a thick cluster of galaxies, it can be destroyed by hot intergalactic gas of the cluster which temperature is of order ten million kelvin. In opposite case a particle can reach another galaxy.

Basically, to resolve the importance of IMP as a material transporters, the questions are about their physical-dynamical characteristics, and impact probabilities. The latter is a subject of our paper. We consider the exoplanets in habitable zones (HZEP) as targets and an IMP as a projectile on a trajectory which can cross a planet orbit, and we are focused on the random probability that an IMP, during its cruise through our Galaxy, will collide with some of HZEP.

2. Materials and Methods

It is well known that the impact probabilities of small projectiles with terrestrial planets in our system are $\lesssim 10^{-8}$. Estimating impact probability for each exoplanet by counting the number of hits onto the collisional sphere with a good statistical accuracy, would require a sample size of $\sim 10^{12}$ or even larger for each of them [20]. Thus, we use a modified approach inspired by previous works on the directed panspermia [21,22]. In addition, we introduced a new feature from the information theory metrics. An IMPs eccentricity depends on its perihelion distance and velocity. The larger its perihelion distance (or larger its velocity relative to the sun), its trajectory would be less modified by gravitational acceleration, while its eccentricity would increase. Thus, very distant IMPs will traverse almost straight lines (i.e., eccentricities converging to infinity) (see [23]). For simplicity, we will assume that IMP follows straight line entering into our Galaxy from position of our solar system.

2.1. Exoplanet Data

At the time of writing, more than 3000 exoplanets have been confirmed (Extrasolar Planets Encyclopaedia, June 2019). The majority of detected planets are with distances of several tens to several thousands pc far away from Sun. Their host star ages are of hundreds of Myr to a few Gyr. For our calculation we needed radius and effective temperature of star, radius (in Jupiter radius R_J) and semimajor axis (in AU) of planet and distance to planetary system (in pc), which yielded the sample of 171 HZEP.

2.2. Habitable Zone

There are several prescriptions how to define HZ and calculate its limits (see an excellent review in [24], and references therein). Usually, the circumstellar (HZ) is assumed to be an annular volume around the star where planets with orbits inside it may be expected to have liquid water on their surface. But for our purpose we calculated HZ as follows: based on polynomial expression for inner and outer limits of HZ given in [25], and effective stellar temperatures collected from EOD, we estimated the effective stellar fluxes. This prescription has been constructed for the stars which effective temperatures correspond to stellar masses between 0.1 and 1.4 M_{\odot} as they are in our sample. Then the HZ limits are given by [26] as

$$d = \left(\frac{L}{L_{\odot}} \right)^{0.5} \frac{1}{S_{\text{eff}}} \text{ AU} \quad (1)$$

where d is either inner or outer limit of HZ, L is the stellar luminosity, L_{\odot} is the luminosity of the present Sun, and S_{eff} is effective stellar flux. Then we estimated the geometric center (cHZ) of HZ as arithmetic mean of inner and outer HZ limits and required that semimajor axis (a) of the planet satisfies following condition

$$|cHZ - a| \leq 0.5 \quad (2)$$

This is very optimistic view. Up to now, the current number of potentially habitable exoplanets detected is about 49 (see <http://phl.upr.edu/projects/habitable-exoplanets-catalog>). This catalog also includes exoplanets up to 10 Earth masses and 2.5 Earth radii to include water-worlds, Mega-Earths, and the uncertainty of radius estimates. Today we have great uncertainty that any exoplanet is really habitable. We suspect that life could depend on many planetary characteristics that are simply not known for exoplanets. Therefore, our criterion is only used to select as large as possible sample of the best objects of interest for our study, not to strictly discriminate the habitable from non habitable worlds.

2.3. Probabilities Estimates

Firstly, using the kernel density estimate (KDE) we obtain the probability distribution of the HZE in the parameter space of the HZE radii and their distances from Earth. Then we estimate impact probabilities by adopting [22] method. Finally, we use information theory metric to evaluate the co-occurrence of two events: planet residence in the HZ and being hit by IMP.

2.3.1. Probability That Planet Is within HZ

Here we describe the process of performing a Kernel density estimation (KDE), a statistical process for density estimation that planet is within HZ. We used the framework of multivariate nonparametric density estimation. In nonparametric statistics no stringent parametric assumptions are made on the underlying probability model that generated the data. The appeal of nonparametric methods are in their ability to reveal structure in data that might be omitted by classical parametric methods.

Let X_1, \dots, X_n be observation drawn independently from an unknown distribution P on R^p with the density f . Kernel density estimates an unknown underlying density f [27] as follows:

$$f_n(x, H) = \frac{1}{n} \sum_{i=1}^n K_H(x - X_i) \tag{3}$$

where $K_H = |H|^{-0.5}K(H^{-0.5}x)$, the matrix H has dimension $p \times p$ is the matrix of smoothing parameters, it is symmetric and positive definite, and $K : \mathbb{R}^p \rightarrow [0, \infty)$ is a probability density. In our case, X_i are two dimensional vectors containing the radii and distances HZE from Earth. Then given a set of data points, KDE interpolates and smooths probability density function on continuous surface using a given kernel. These two aspects are relevant for our investigation, due to sparse data. The matrix H also controls the bandwidth of kernel. In machine learning contexts, the hyperparameter tuning often is done empirically via a cross-validation approach. Since the radius of planets and their distances varies over several order of magnitudes, for bandwidth estimate we used cross validation least squares method. Then, the probability density function (PDF) is evaluated in a grid of points covering the region of analysis. In practice we construct a grid of 800×800 points.

2.3.2. Evaluating Collision Probability

We consider IMP of negligible dimension and target planets that are massive enough to induce gravitational focusing at close encounters. Here we consider the probability of capture of IMP within kinematical framework suggested by [22,28,29] for directed panspermia. This approach uses the proper motions of the targets, their distances and the velocity of projectile. Combined the positional uncertainty and dimension of the target object permit calculating the probability of hitting. The positional uncertainty δy of the target at arrival time of projectile is given by following equation

$$\delta y = 1.5 \times 10^{-13} \alpha \frac{d^2}{v} \tag{4}$$

where α is the resolution of proper motion of the target object, d is distance from the Earth and v is velocity of the projectile. We set $\alpha = 10^{-5}$ as suggested by [28,29].

The probability that projectile hits the target area A_t of radius r_t is given by

$$P_t = \frac{A_t}{\pi(\delta y)^2} = 4.4 \times 10^{25} \frac{r_t^2 v^2}{\alpha^2 d^4} \tag{5}$$

For planetary system the area A_t may be even the width of HZ. For very large impactor initial velocities (v_∞), as it is case of IMP, the impact parameter $b = R(1 + \frac{2GM}{Rv_\infty^2})^{0.5}$ (where G is gravitational constant) tends to planet’s radius R , while the planet mass M does not play any role as it can be seen. Thus, we will use the radius of an exoplanet to estimate A_t . Note that in Equation (4) we employ the Earth-exoplanet distance. However, the probability calculated with Equation (5) is valid not only for Earth-exoplanet direction but for any point on the sphere which radius is Earth-exoplanet distance and center in the exoplanet.

2.3.3. Information Theory Metrics

In order to evaluate the statistical variability of the hitting a planet within HZ by IMP, we utilize the information theory metrics of entropy. The aim of this metric is to evaluate the co-occurrence of both planet residence in HZ and being hit by IMP. Entropy can express the mean of information that an event provides when it takes place, the uncertainty about the outcome of an event and the dispersion of the probabilities with which the events take place. Here, we first recall the definition of the Shannon entropy. Let we consider a set of planets S , whose are considered as a sample on a vector random variable $X \in R^d$, with an associated probability density function describing their distribution. This

PDF $p(X = x)$ estimates the probability of an observation x on X , denoted as $p(X)$. We evaluate the Shannon's information entropy [30] as

$$H(X) = - \sum_{k=1}^d p(x_k) \log p(x_k) \quad (6)$$

The entropy $H(X)$ provides a measure of the information content in the probability spectrum [31]. The joint Shannon entropy of a set of independent random variables is sum of their individual entropies. In opposite case, the total entropy is a sum of conditional entropies.

In this sense, let $V = \{V_j | j = 1, \dots, m\}$ is a vector of probabilities obtained by concatenation of probability vectors estimated by Equations (3) and (5). The event that planet is found within HZ and being hit by IMP are independent and their co-occurrence is given by

$$EI = \frac{- \sum_{j=1}^k V_j \log V_j}{\log k} \quad (7)$$

where k is the number of probability distributions used to create V (in our case two). Since Shannon's entropy can take value $H(X) \in [0, \log(n)]$, the EI is positive definite and normalized. The higher value of EI means the higher co-occurrence of the events. Also this metric can be seen as a reflection of the level of concentration of such events. Since Shannon entropy may be used globally, for the whole data or locally to evaluate entropy of probability density distributions around some points, the same is valid for EI as well. So this quality of Shannon entropy can be generalized to estimate importance of specific events, e.g., rare events [32].

3. Results

Since the impact probabilities are calculated within the phase space of planets radii and their distances from Earth, we choose the same phase space for depicting HZ probability map. In Figure 1 we show the probability map of habitability, obtained at each point of the plane determined by radius and distance of planet from Earth. The results show that the hot zones of habitability is bellow 600 pc and $0.3 R_j$, but the prominent spots are bellow distances of 400 pc, and planet's radii of $0.2 R_j$. There are large regions of parameter space where it is unlikely that planets resides within HZ because simply that part of parameter space is not populated by exoplanets in our sample.

Next, we calculated the probabilities of exoplanets from our sample being hit by an IMP. We considered that IMP enters into our Galaxy within vicinity of our Solar system. Its velocity is taken as 300 km s^{-1} . The probability map of hitting are in the form of stripes (see Figure 2). The logarithmic scale is used for the color-coding which allows greater detail to be seen in regions where the probabilities are low. The 'hot zone' is within 200 pc and it is spread evenly across the values of radii of exoplanets. However the probabilities are decreasing gradually with the distance.

Figure 3 reveals emerging pattern of areas with concentrated events of exoplanets within HZ being hit by IMP. Note that hotspots are determined by event density and not event counts. The unit of analysis is defined from the grid of dimension of 800×800 cells in phase space. Thus a hotspot can be created from very few small probability if they are concentrated in a small area. It also assists with identifying clusters of key populations of planets. The clustering is increasing toward the inner part of Galaxy, and the radii of planets are bellow $0.5 R_j$. This feature can be amplified if the majority of planets bearing life are spread towards the inner part of the Galaxy, as suggested by [33].

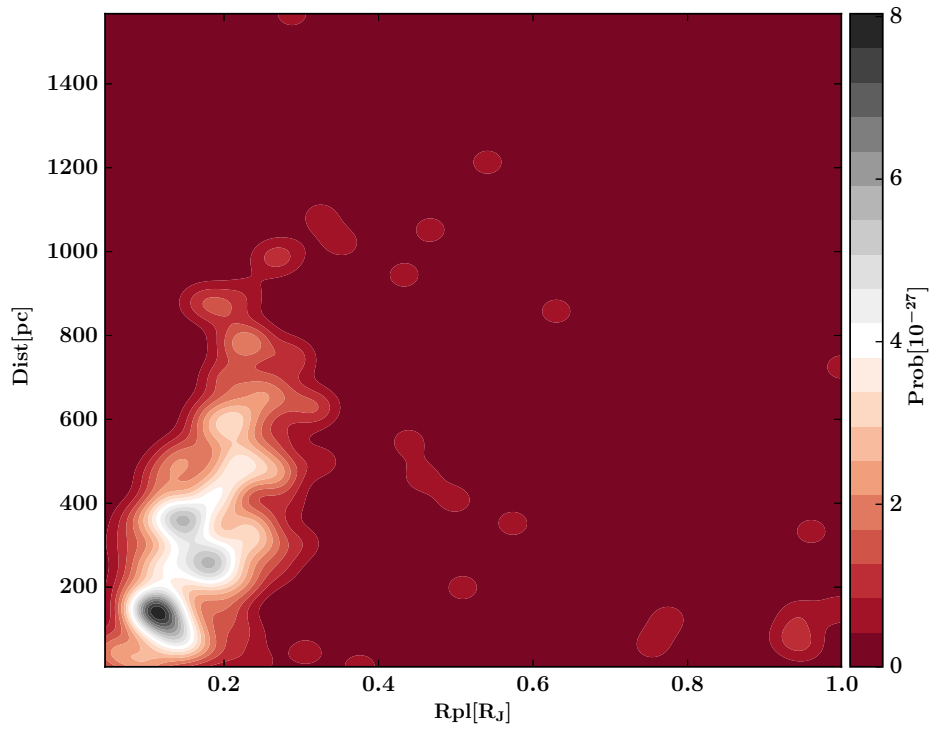


Figure 1. The HZ probability in the phase space of radius (x axis in Jupiter radii) and distance of planet from Earth (y axis in parsecs). The contour levels correspond to the HZ probability as indicated on the color bars. Note the small values of probability, since we used non-parametric KDE.

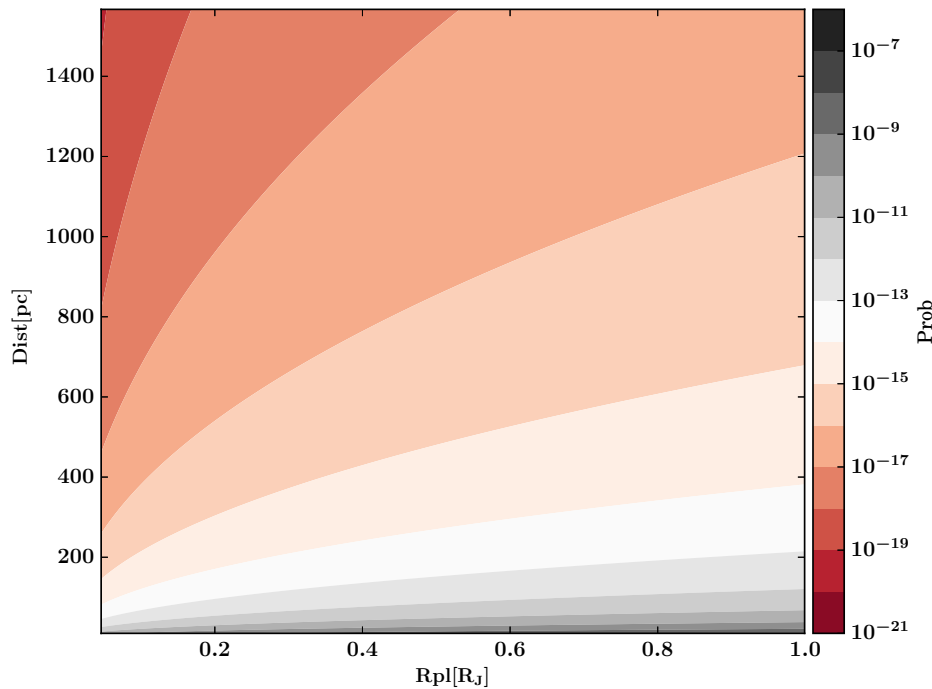


Figure 2. The probability that exoplanets within our sample are hit by an IMP. The axes are the same as in Figure 1. The contour levels correspond to the probability of hitting as indicated on the color bars.

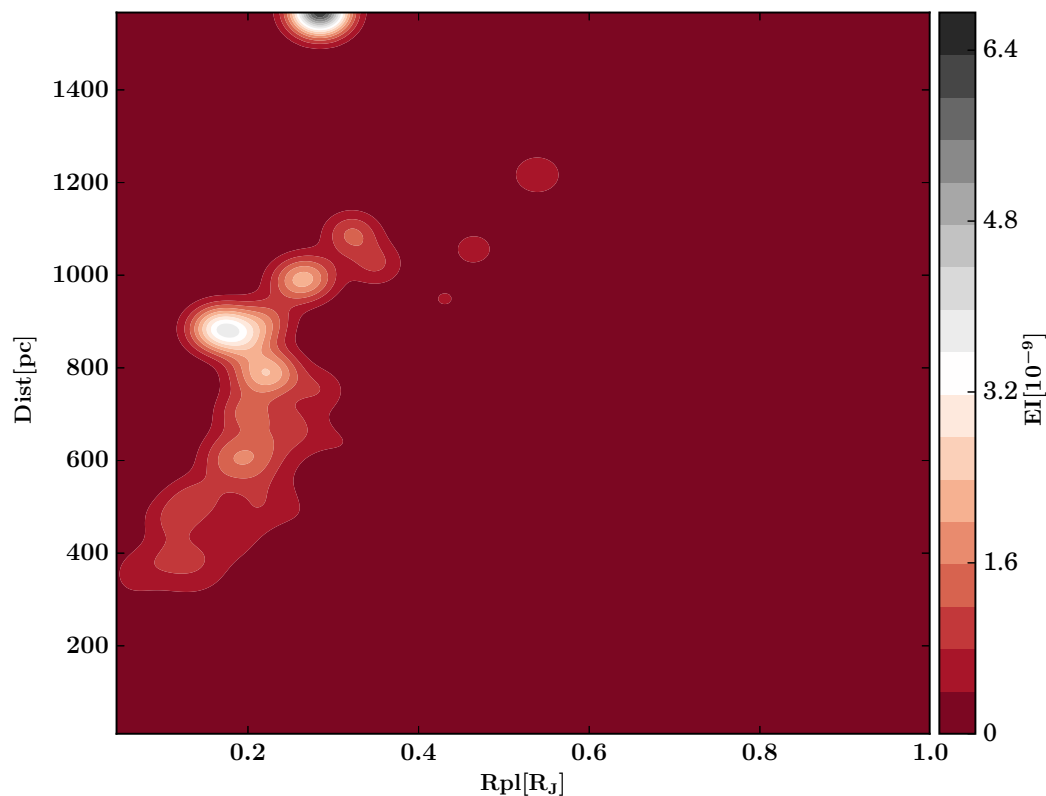


Figure 3. The statistical map of co-occurrence of events that exoplanet is in the HZ and being hit by IMP. The axes are the same as in Figure 1. The contour levels correspond to the probability of hitting as indicated on the color bars. A logarithmic scale is used for the color-coding.

4. Discussion

The lack of data to estimate the probability of an event accurately is not only problem. In undersampled regime we may fail to detect all events with probabilities greater than zero. In general, estimating a distribution in this setting is a difficult. Contrary, estimating the entropy, is easier. In fact, in many cases, entropy can be accurately estimated with fewer sample.

Even using relatively small sample of exoplanets, the data demonstrated that EI is robust and sensitive measure for differentiating hot spots for IMP's collision. The map is not based on any particular assumption about the distribution of the exoplanets parameters, however we assumed the IMP entered into our Galaxy within the vicinity of our planet.

The EI was stable in nearly the whole phase space defined by radius and planet - Earth distance except several aggregates within the range of distances 400–1200 pc and radii below 0.4 R_J . This region is characterized by a clear distribution and a sharp contrast.

Comparison with well known impact probabilities with terrestrial planets, which are not larger than $\lesssim 10^{-8}$ [20], indicates that our estimates of probabilities of IMP impacts with exoplanets within HZ are realistic.

Perhaps there are many mechanism which can increase IMP impact probabilities, but we will concentrate on only one due to underlying observations. Importantly, the IMP could decelerate in the vicinity of evaporating planets, whose outer layers are lifted into the surrounding space forming large clouds. For example, KIC 12557548 b is assumed to be a rocky planet more massive than Mercury, with a surface temperature of ~ 2100 K, which completes an entire orbit in just 16 h. These extreme dynamical and physical properties cause a continuous loss of material, forming an extended tail of dust following the planet in its orbital path [34]. An IMP, after collision with particles in such clouds, could be fragmented [35]. In such case, the probability of IMP fragments impacts would increase.

Next, we consider the amount of possible organic content in IMP. Assuming it is a chondrit, probably carbonaceous, an estimated density of such chondrites can be taken between 2.3 and 2.5 g cm⁻³ [36]. Thus, the mass of IMP could be 10⁻⁵ g which is relatively close to a mass inferred by [7]. Taking into account that about 2% of such bodies mass can be organic [37], we estimate that the mass of possible biotic content in IMP is about 10⁻⁶ g. There is a further question: would IMP mass m_{res} satisfy biomass requirements according to [21] equation:

$$m_{biom} = m_{res} \frac{c_{res}}{c_{biom}} \quad (8)$$

where m_{biom} is the amount of biomass constructed from m_{res} of resource material, c_{res} is a concentration of essential elements (C, H, N, O, P, S, Ca, Mg i K) in the resource material, c_{biom} is the concentration of essential elements in a given biomass. Here we used standard values for $m_{biom} = 10^{-10}$ kg [22], $c_{res} = 973.3$ g kg⁻¹, $c_{biom} = 180.763$ g kg⁻¹ [21]. Plugging these values in Equation (8), the $m_{res} = 5.7 \times 10^{-7}$ g is obtained. From comparison with the inferred mass of IMP 10⁻⁵ – 10⁻³ g one can see that IMP is potentially viable vehicle for organic material transfer. The second question here is which and how complex organic molecules can be transported by IMP. To answer this question, it helps to recall that the unidentified infrared emission (UIE) bands have been detected in planetary nebulae, reflection nebulae, HII regions, diffuse interstellar medium, and even in other galaxies (see [38], and references therein). Moreover, up to 20% of total luminosity of some active galactic nuclei is emitted in the UIE bands [39]. UIE bands detected in quasars [40] and in high-redshift galaxies [41] imply that complex organic species were widespread as early as 10 billion years ago. Thus, abiological synthesis of complex organics has been occurring through most of the Universe history. Different chemical species have been suggested as sources of the UIE bands: from PAH molecules [42], small carbonaceous molecules [43], hydrogenated amorphous carbon, soot and carbon nanoparticles [44], quenched carbonaceous composite particles [45], kerogen and coal [46], petroleum fractions [47], up to mixed aromatic or aliphatic organic nanoparticles [48]. Among these, the PAH hypothesis is the most popular, but has a number of difficulties and its validity has been questioned [49].

To determine the probable spatial upper boundary on material migration on intergalactic scale, we can use as upper velocity limit for fragment ejected by galaxies a recoil velocity in the final stage of supermassive-binary coalescence. Numerical relativity simulations produced recoil velocities ~10³ km s⁻¹, even 5 × 10³ km s⁻¹ (see [50], and references there in). Moreover, Robinson et al. [51] using spectropolarimetric observations of E1821+643 found that the central supermassive black hole is moving with a velocity ~2100 km s⁻¹ relative to the host galaxy, that implies a gravitational recoil following the merger of a supermassive black hole binary system. Thus, we can choose upper velocity limit of 3000 km s⁻¹ which is 1% of light velocity. Consequently, exchange of material over 13 billion years of Universe lifespan could happen over distances of 130 × 10⁶ light years. The radius of Universe is about 45 × 10⁹ light years [52], so a material transfer could occur within 0.22% of the observable Universe radius. Conselice et al. [53] found that the total number of galaxies is 2.8 ± 0.6 × 10¹² in observable Universe, which means that 616 × 10⁷ galaxies could exchange material. One can anticipate, high efficient material transfer occurring within a galaxy cluster (containing between 100 and 1000 galaxies). Milky Way is not a member of any cluster, so the material exchange could probably occur only within our Local Group of Galaxies.

Some Parallels with Biological Immigration Models

The immigration of the material from space is similar, to some extent, to a population linear model of birth-death-immigration with binomial catastrophes [54]. We can assume that we have a population of molecules on our planet, which can be terminated or give birth to other molecules and in addition there are immigrant molecules. The model considers a continuous time Markov chain $N(t) : t \geq 0$ with state space $N_0 = 0, 1, 2 \dots$ and an initiator defined as:

$$q_{ij} = \begin{cases} i\lambda + \nu & \text{if } j = i + 1, i \geq 0 \\ \binom{i}{j} p^j (1 - p)^{i-j} \gamma + i\mu \delta_{i-1} & \text{if } j = 0, \dots, i, i \geq 0 \end{cases} \quad (9)$$

where δ_{i-1} is delta Kronecker symbol. Thus, the transition of stochastic process $N(t)$ from state i to state j occurs as follows: the upper branch resembles the individual up-leap associated with an immigration Poisson process at rate ν and the individual births (creation of molecules) occurring at rate λ . Moreover there exist two types of extinctions-natural death and random catastrophe mechanism. So the rate $q_{i,i-1} = i\mu$ is related to the individual death mechanism where the life time of molecule is terminated after an exponentially distributed random time at rate μ . And second down rate occurs due to catastrophic events $q_{ij} = \binom{i}{j} p^j (1 - p)^{i-j} \gamma$. Catastrophes appear as a Poisson process at rate γ .

In Figure 4 is given transient distribution as time evolves for state 0 while the birth rate is $\lambda = 1$, the immigration rate is $\nu = 1$, the death rate is $\mu = 3$, the survival probability is $p = 0.5$ and the catastrophe occurrence rate is $\gamma = 0.000001$.

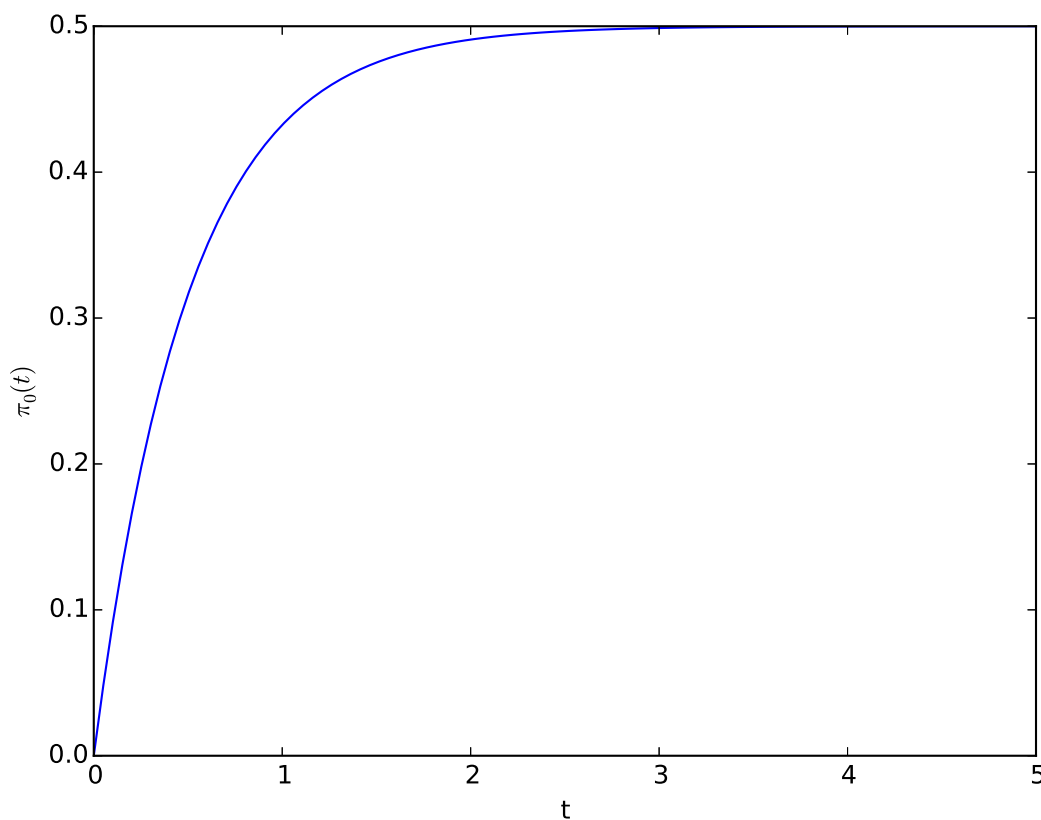


Figure 4. The transient distribution of birth/immigration-death process with binomial catastrophes for state 0.

5. Conclusions

First, we give the probability distribution of exoplanets in HZ. Second we estimate probabilities of IMP impacts with exoplanets. Third we estimate probability of cooccurrence of exoplanets being in HZ and hit by IMP. The entropy hot spots of IMP impacts are correlated with the dimension of planets. The clustering is increasing toward the inner region of Galaxy. This feature can be amplified if the majority of planets bearing life are spread towards the inner part of the Galaxy. The forth, we estimate that IMP mass (10^{-5} g) under assumption it is a chondrit and its potential biological content mass of (10^{-6} g). Thus, such IMP satisfies Mautner criterion for insemination. The fifth, on the analogy with the theory of immigration, we estimate the transient distribution for birth/death/immigration process of molecules for the simplest case.

Finally, the methodology and findings are of novel interest for the following reasons. The EI helps us to compare the concentration rate of events which are not frequent and tend to be highly concentrated by taking into account the random nature of such events. Moreover, it detects structural changes in the considered phase and it can be used to compare different regions of exoplanets phase space.

Funding: This research received no external funding.

Acknowledgments: The author sincerely thank to the Referee for the constructive comments and recommendations which definitely improve the quality of the paper. This work is supported by project (176001) Astrophysical Spectroscopy of Extragalactic Objects.

Conflicts of Interest: The author declare no conflicts of interest.

References

1. Newman, M.E.J. Power Laws, Pareto Distributions and Zipf's Law. *Contemp. Phys.* **2005**, *46*, 323–351. [[CrossRef](#)]
2. Zolotov, M.Y.; Shock, E.L. Stability of Condensed Hydrocarbons in the Solar Nebula. *Icarus* **2001**, *150*, 323–337. [[CrossRef](#)]
3. Fraser, H.J.; McCoustra, M.R.S.; Williams, D.A. The molecular universe. *Astron. Geophys.* **2002**, *43*, 10–18. [[CrossRef](#)]
4. Meech, K.J.; Weryk, R.; Micheli, M.; Kleyna, J.T.; Hainaut, O.R.; Jedicke, R.; Wainscoat, R.J.; Chambers, K.C.; Keane, J.V.; Petric, A.; et al. A brief visit from a red and extremely elongated interstellar asteroid. *Nature* **2017**, *552*, 378–381. [[CrossRef](#)] [[PubMed](#)]
5. Belbruno, E.; Moro-Martin, A.; Malhotra, R.; Savransky, D. Chaotic Exchange of Solid Material between Planetary Systems: Implications for Lithopanspermia. *Astrobiology* **2012**, *12*, 754–774. [[CrossRef](#)] [[PubMed](#)]
6. Taylor, A.D.; Baggaley, W.J.; Steel, D.I. Discovery of interstellar dust entering the Earth's atmosphere. *Nature* **1996**, *380*, 323–325. [[CrossRef](#)]
7. Afanasiev, V.L.; Kalenichenko, V.V.; Karachentsev, I.D. Detection of an Intergalactic Meteor Particle with the 6-m Telescope. *Astrophys. Bull.* **2007**, *62*, 301–397. [[CrossRef](#)]
8. Taylor, A.D.; Baggaley, W.J.; Bennett, R.G.T.; Steel, D.I. Radar measurements of very high velocity meteors with AMOR. *Planet. Space Sci.* **1994**, *42*, 135–140. [[CrossRef](#)]
9. Musci, R.; Weryk, R.J.; Brown, P.; Campbell-Brown, M.D.; Wiegert, P.A. An Optical Survey for Millimeter-sized Interstellar Meteoroids. *Astrophys. J.* **2012**, *745*, 161. [[CrossRef](#)]
10. Swift, J.J.; Johnson, J.A.; Morton, T.D.; Crepp, J.R.; Montet, B.T.; Fabrycky, D.C.; Muirhead, P.S. Characterizing the Cool KOIs. IV. Kepler-32 as a Prototype for the Formation of Compact Planetary Systems throughout the Galaxy. *Astrophys. J.* **2013**, *764*, 105. [[CrossRef](#)]
11. Meyer, C.; Fritz, J.; Migaiski, M.; Stöffler, D.; Artemieva, N.A.; Hornemann, U.; Moeller, R.; De VERA, J.P.; Cockell, C.; Horneck, G.; et al. Shock experiments in support of the Lithopanspermia theory: The influence of host rock composition, temperature, and shock pressure on the survival rate of endolithic and epilithic microorganisms. *Meteorit. Planet. Sci.* **2011**, *46*, 701–718. [[CrossRef](#)]
12. Berera, A. Space Dust Collisions as a Planetary Escape Mechanism. *Astrobiology* **2017**, *17*, 1274–1282. [[CrossRef](#)] [[PubMed](#)]
13. Scharf, C.; Cronin, L. Quantifying the origins of life on a planetary scale. *Proc. Natl. Acad. Sci. USA* **2016**, *113*, 8127–8132. [[CrossRef](#)] [[PubMed](#)]
14. Ginsburg, I.; Lingam, M.; Loeb, A. Galactic Panspermia. *Astrophysical J. Lett.* **2017**, *868*, L12–L21. [[CrossRef](#)]
15. Setiawan, J.; Klement, R.; Henning, T.; Rix, H.W.; Rochau, B.; Rodmann, J.; Schulze-Hartung, T. A giant planet around a metal-poor star of extragalactic origin. *Science* **2010**, *330*, 1642–1644. [[CrossRef](#)] [[PubMed](#)]
16. Draine, B.T. Interstellar Dust Grains. *Annu. Rev. Astron. Astrophys.* **2003**, *41*, 241–289. [[CrossRef](#)]
17. Tarafdar, S.P.; Wickramasinghe, N.C. Effects of Suprathermal GrainsSolid state astrophysics. In *Solid State Astrophysics, Proceedings of a Symposium Held at the University College, Cardiff, Wales, 9–12 July 1974*; Wickramasinghe, N.C., Morgan, D.J., Eds.; D. Reidel Publishing Company: Dodrecht, The Netherlands, 1976; pp. 249–260.

18. Adam, R.; Ade, P.A.R.; Aghanim, N.; Ashdown, M.; Aumont, J.; Baccigalupi, C.; Banday, A.J.; Barreiro, R.B.; Bartolo, N.; Battaner, E.; et al. Planck intermediate results XLIII. Spectral energy distribution of dust in clusters of galaxies. *Astron. Astrophys.* **2016**, *596*, A104.
19. Yamada, K.; Kitayama, T. Infrared Emission from Intracluster Dust Grains and Constraints on Dust Properties. *MNRAS* **2005**, *57*, 611–619. [[CrossRef](#)]
20. Rickman, H.; Wisniowski, T.; Wajer, P.; Gabryszewski, R.; Valsecchi, G.B. Monte Carlo methods to calculate impact probabilities. *Astron. Astrophys.* **2014**, *569*, 1–15. [[CrossRef](#)]
21. Mautner, M.N. Life in the Cosmological Future: Resources, Biomass and Populations. *J. Br. Interplanet. Soc.* **2005**, *58*, 167–180.
22. Mautner, M.; Matloff, G.L. A technical and ethical evaluation of seeding nearby solar systems. *J. Br. Interplanet. Soc.* **1979**, *32*, 419–423.
23. Engelhardt, T.; Jedicke, R.; Vereš, P.; Fitzsimmons, A.; Denneau, L.; Beshore, E.; Meinke, B. An Observational Upper Limit on the Interstellar Number Density of Asteroids and Comets. *Astron. J.* **2017**, *153*, 133. [[CrossRef](#)]
24. Gallet, F.; Charbonnel, C.; Amard, L.; Brun, S.; Palacios, A.; Mathis, S. Impacts of stellar evolution and dynamics on the habitable zone: The role of rotation and magnetic activity. *Astrophys. J.* **2017**, *597*, A14. [[CrossRef](#)]
25. Underwood, D.R.; Jones, B.W.; Sleep, P.N. The evolution of habitable zones during stellar lifetimes and its implications on the search for extraterrestrial life. *Int. J. Astrobiol.* **2003**, *4*, 289–299. [[CrossRef](#)]
26. Kasting, J.F.; Whitmire, D.P.; Reynolds, R.T. Habitable Zones around Main Sequence Stars. *Icarus* **1993**, *101*, 108–128. [[CrossRef](#)] [[PubMed](#)]
27. Wand, M.P.; Jones, M.C. *Kernel Smoothing*; CRC Monographs on Statistics & Applied Probability (60); Chapman & Hall: Boca Raton, FL, USA, 1995; pp. 1–208.
28. Mautner, M.N. Directed Panspermia. 2. Technological Advances Toward Seeding Other Solar Systems, and the Foundations of Panbiotic Ethics. *J. Br. Interplanet. Soc.* **1995**, *48*, 435–440.
29. Mautner, M.N. Directed panspermia. 3. Strategies and motivation for seeding star-forming clouds. *J. Br. Interplanet. Soc.* **1997**, *50*, 93–102.
30. Shannon, C.E. A Mathematical Theory of Communication. *Bell Syst. Tech. J.* **1948**, *27*, 379–423. [[CrossRef](#)]
31. Consolini, G.; Tozzi, R.; De Michelis, P. Complexity in the sunspot cycle. *Astron. Astrophys.* **2009**, *506*, 1381–1391. [[CrossRef](#)]
32. Maszczyk, T.; Duch, W. Comparison of Shannon, Renyi and Tsallis Entropy used in Decision Trees. In *Artificial Intelligence and Soft Computing ICAISC*; Rutkowski, L., Tadeusiewicz, R., ZadehJacek, L.A., Zurada, M., Eds.; Springer: Berlin/Heidelberg, Germany, 2008; pp. 643–651.
33. Gowanlock, M.G.; Patton, D.R.; McConnell, S. A model of habitability within the Milky Way Galaxy. *Astrobiology* **2011**, *11*, 855–873. [[CrossRef](#)]
34. Bochinski, J.J.; Haswell, C.A.; Marsh, T.R.; Dhillon, V.S.; Littlefair, S.P. Direct evidence for an evolving dust cloud from the exoplanet KIC 12557548 b. *Astrophys. J. Lett.* **2015**, *800*, L21–L27. [[CrossRef](#)]
35. Napier, W.M. A mechanism for interstellar panspermia. *Mon. Not. R. Astron. Soc.* **2004**, *348*, 46–51. [[CrossRef](#)]
36. Britt, D.T.; Consolmagno, G.J. Stony meteorite porosities and densities: A review of the data through 2001. *Meteorit. Planet. Sci.* **2003**, *38*, 1161–1180. [[CrossRef](#)]
37. Sephton, M.A. Organic matter in ancient meteorites. *Astron. Geophys.* **2004**, *45*, 8–14. [[CrossRef](#)]
38. Kwok, S. Complex organics in space from Solar System to distant galaxies. *Astron. Astrophys. Rev.* **2016**, *24*, 1–8. [[CrossRef](#)]
39. Smith, J.D.T.; Draine, B.T.; Dale, D.A.; Moustakas, J.; Kennicutt, R.C., Jr.; Helou, G.; Armus, L.; Roussel, H.; Sheth, K.; Bendo, G.J.; et al. The mid-infrared spectrum of star-forming galaxies: Global properties of polycyclic aromatic hydrocarbon emission. *Astrophys. J.* **2007**, *656*, 770–791. [[CrossRef](#)]
40. Lutz, D.; Sturm, E.; Tacconi, L.J.; Valiante, E.; Schweitzer, M.; Netzer, H.; Maiolino, R.; Andreani, P.; Shemmer, O.; Veilleux, S. PAH emission and star formation in the host of the $z \sim 2.56$ QSO. *Astrophys. J. Lett.* **2007**, *661*, L25–L28. [[CrossRef](#)]
41. Teplitz, H.I.; Desai, V.; Armus, L.; Chary, R.; Marshall, J.A.; Colbert, J.W.; Frayer, D.T.; Pope, A.; Blain, A.; Spoon, H.W.W.; et al. Measuring PAH emission in ultra-deep Spitzer IRS spectroscopy of high-redshift IR-luminous galaxies. *Astrophys. J.* **2007**, *659*, 941–949. [[CrossRef](#)]
42. Léger, A.; Puget, J.L. Identification of the unidentified IR emission features of interstellar dust? *Astron. Astrophys.* **1984**, *137*, L5–L8.

43. Bernstein, L.S.; Lynch, D.K. Small carbonaceous molecules, ethylene oxide and cyclopropenylidene: Sources of the unidentified infrared bands? *Astrophys. J.* **2009**, *704*, 226–239. [[CrossRef](#)]
44. Hu, A.; Duley, W.W. Spectra of carbon nanoparticles: Laboratory simulation of the aromatic CH emission feature at 3.29 μm –3.29 μm . *Astrophys. J. Lett.* **2008**, *677*, L153–L156. [[CrossRef](#)]
45. Sakata, A.; Wada, S.; Onaka, T.; Tokunaga, A.T. Infrared spectrum of quenched carbonaceous composite (QCC). II—A new identification of the 7.7 and 8.6 micron unidentified infrared emission bands. *Astrophys. J.* **1987**, *320*, L63–L67. [[CrossRef](#)]
46. Papoular, R.; Conrad, J.; Giuliano, M.; Kister, J.; Mille, G. A coal model for the carriers of the unidentified IR bands. *Astron. Astrophys.* **1989**, *217*, 204–208.
47. Cataldo, F.; Keheyan, Y.; Heymann, D. A new model for the interpretation of the unidentified infrared bands (UIBS) of the diffuse interstellar medium and of the protoplanetary nebulae. *Int. J. Astrobiol.* **2002**, *1*, 79–86. [[CrossRef](#)]
48. Kwok, S.; Zhang, Y. Unidentified infrared emission bands: PAHs or MAONs? *Astrophys. J.* **2013**, *771*, 5. [[CrossRef](#)]
49. Zhang, Y.; Kwok, S. On the viability of the PAH model as an explanation of the unidentified infrared emission features. *Astrophys. J.* **2015**, *798*, 37. [[CrossRef](#)]
50. Lena, D.; Robinson, A.; Marconi, A.; Axon, D.J.; Capetti, A.; Merritt, D.; Batcheldor, D. Recoiling supermassive black holes: A search in the nearby Universe. *Astrophys. J.* **2015**, *795*, 146. [[CrossRef](#)]
51. Robinson, A.; Young, S.; Axon, D.J.; Kharb, P.; Smith, J.E. Spectropolarimetric Evidence for a Kicked Supermassive Black Hole in the Quasar E1821+643. *Astrophys. J. Lett.* **2010**, *717*, L122–L126. [[CrossRef](#)]
52. Gott, J.R., III; Jurić, M.; Schlegel, D.; Hoyle, F.; Vogeley, M.; Tegmark, M.; Bahcall, N.; Brinkmann, J. A Map of the Universe. *Astrophys. J.* **2005**, *624*, 463–484.
53. Conselice, C.J.; Wilkinson, A.; Duncan, K.; Mortlock, A. The evolution of galaxy number density at $z < 8$ and its implications. *Astrophys. J.* **2016**, *830*, 83.
54. Kapodistria, S.; Phung-Duc, T.; Resing, J. Linear Birth/Immigration-Death Process with Binomial Catastrophes. *Probab. Eng. Informational Sci.* **2015**, *30*, 79–111. [[CrossRef](#)]



© 2019 by the author. Licensee MDPI, Basel, Switzerland. This article is an open access article distributed under the terms and conditions of the Creative Commons Attribution (CC BY) license (<http://creativecommons.org/licenses/by/4.0/>).